Stripe patterns in two-dimensional systems with core-corona molecular architecture

Gianpietro Malescio and Giuseppe Pellicane
Dipartimento di Fisica, Università di Messina and Istituto Nazionale di Fisica della Materia, 98166 Messina, Italy
(Received 11 November 2003; published 11 August 2004)

The behavior of a two-dimensional system of particles interacting through a potential consisting of a hard core surrounded by a soft repulsive corona is investigated at several densities and temperatures. We find that the competition between hard and soft repulsions gives origin to the spontaneous formation of spatial patterns resembling stripe textures. The effect of varying the hard and soft core radii ratio as well as that of adding an attractive component to the interparticle interaction is studied. The model investigated is relevant for macromolecular topologies possessing two intrinsic length scales.

DOI: 10.1103/PhysRevE.70.021202 PACS number(s): 61.20.Gy, 61.25.Em

I. INTRODUCTION

Spontaneous formation of stripe phases often occurs in two-dimensional systems as the result of self-organization processes. Materials showing such behavior include Langmuir monolayers [1], magnetic films [2], lipid monolayers [3], liquid crystals [4], polymer films [5], etc. Possible technological applications of such nanostructures as nanolithography and nanoelectricity, motivate interest in studying the physical mechanisms underlying the phenomenon. Stripe formation is usually attributed to the competition between short-range attractive forces and long-range repulsion arising from dipole interactions [6,7]. Recently, however, it was shown through numerical simulation that stripe phases may arise also in the presence of purely repulsive short-ranged interactions with two characteristic distances [8]. Such feature is present in physical systems with core-corona architecture, such as dendritic polymers, hyper-branched star polymers, diblock copolymers, etc., which are characterized by two repulsive length scales, related to the hard and soft repulsions, respectively. For instance, diblock copolymers suspended in decane [9] self-assemble to produce soft spherical micelles with a dense core and a diffuse corona. By varying the degree of polymerization or the aggregation number, it is possible to tune the length scale of each block. A similar topology characterizes another family of macromolecules recently synthesized, i.e., dendrimer compounds consisting of a compact poly(benzylether) core segment decorated with a diffuse corona of dodecyl chains [10]. These dendrimers self-assemble in spherical micelles with a compact core of benzylether rings and a floppy, squishy corona of alkaly chains. The interaction between core-corona micelles is primarily steric, i.e., repulsive and short-range. The micellar architecture suggests that the potential is characterized by three regimes. At large distances, the micelles do not overlap and the interaction vanishes. As the coronas begin to overlap, the entropy of the brush-like coronas decreases, which gives rise to an effective soft repulsion between the micelles. Finally, at small separations penetration of compact cores is very unfavorable and gives rise to hard-core repulsion. This picture is in qualitative agreement with recent, detailed molecular dynamics simulations [11].

The effectiveness of each length scale depends on the thermodynamic conditions. At large pressure and temperature the effective repulsive distance is the hard-core radius, whereas at small pressure and temperature the effective repulsive distance is the soft-core radius. Between these two regimes there is a thermodynamic region in which the two distances are both partially effective. This subtle form of competing interactions may yield domain formation. Here we continue and extend the investigation, begun in Ref. [8], of the behavior of a two-dimensional (2D) system of particles consisting in a hard core and a soft repulsive corona. We find that at densities where the hard and soft core radii compete with each other, the system undergoes, upon decreasing the temperature, a transition to a lamellar or labyrinthine phase. This behavior is substantially unaltered by variations of the two repulsive distances, at least so far as they remain comparable, and is robust upon the introduction of an attractive component in the interaction potential.

II. MODEL AND METHODS

Core-corona architectures may be modeled through intermolecular potentials with a hard core plus a repulsive shoulder (softened-core potentials). The infinite repulsion is due to the impenetrability of the electronic shells. The finite repulsion represents the combination of all the quantum and classical repulsive effects averaged over the angular part. Softened-core potentials with attractive interactions at large distances were first proposed by Stell and Hemmer [12] to understand the possibility of a solid-solid critical point in materials as Ce and Cs. Similar potentials were later used to rationalize the properties of liquid metals, alloys, electrolytes, colloids, and the water anomalies [13–24].

Here we consider a model system of particles interacting through a purely repulsive radially symmetric pair potential $U(r)$ which consists of an impenetrable hard-core of diameter σ_0 plus a repulsive square shoulder of finite height (soft core) extending to $r=\sigma_1$:

$$U(r)=\begin{cases}\infty & \text{for } r<\sigma_0\\ U_R & \text{for } \sigma_0\leqslant r<\sigma_1\\ 0 & \text{for } \sigma_1\leqslant r,\end{cases} \tag{1}$$

where r is the pair distance and $U_R>0$ is the finite (soft-core) repulsive energy. Our model potential presents two

characteristic short-range repulsive distances: σ_0, associated with the hard-core exclusion between two particles, and σ_1, associated with the weak repulsion generated by the soft core. Choosing σ_0 and U_R as length and energy units, respectively, our model depends only on one parameter, i.e., the ratio $R=\sigma_1/\sigma_0$. We initially choose $R=2.5$.

Monte Carlo (MC) calculations are performed with a standard Metropolis algorithm in a square box with square periodic boundaries. *NVT* simulations are performed with $N=1000$ particles (check runs with $N=2000$, 4000 were also done with no significant changes in the quantities monitored). Equilibration cycles consist, for each thermodynamic state, of at least 10^6 MC steps (each step consisting of an attempt to move all the particles, acceptance rate between 0.4 and 0.5). The structure factor is calculated as the Fourier transform of the density-density correlation function through cumulation runs of $2\times10^4-10^5$ MC steps (depending on the density). *NPT* simulations are performed with $N=500$ (check runs with $N=1000$ were done with no significative changes in the quantities monitored).

III. GEOMETRICAL ANALYSIS

The phase diagram of the model considered is expected to be characterized by multiple crystalline structures [23]. It is then useful to perform a preliminary analysis of the possible structural arrangements of the system. At $T=0$ the thermodynamically stable configuration of the system is the one which minimizes the enthalpy. However, it is not possible to safely identify, for each pressure, the structure of lowest enthalpy. The usual approach is to compare the enthalpies of different structures (cubic, tetragonal, hexagonal, etc.) using simulated annealing techniques to guess the possible crystalline lattices. Here, we use geometrical considerations to rapidly figure out which are the relevant densities for the system, although a close correspondence with finite temperature configurations should not be necessarily expected. The different packing geometries can be classified according to the relevant crystal lattice (square, rectangular, or triangular); we will further distinguish among rectangular lattices according to the lattice parameters $d_\perp$ and $d_\parallel$, where the suffixes stand for perpendicular and parallel to the stripe direction, respectively. The basic elements may be simple particles, dimers (couples of particles with touching hard cores and partially overlapping coronas), trimers (triplets of particles whose hard cores are in contact with each other).

Figure 1 illustrates a number of configurations that can be realized by the system at different densities (in the following, density is expressed in units of $1/\sigma_0^2$). Figure 1(a) shows a square lattice of particles ($d_\perp=d_\parallel=\sigma_1$, $\rho=(\sigma_0/\sigma_1)^2=0.16$). Figure 1(b) shows a triangular lattice of particles ($\rho=(2\sqrt{3}/3)(\sigma_0/\sigma_1)^2\approx0.184$ [25]). This is the densest arrangement attainable without interpenetration of coronas. Figure 1(c) shows a rectangular lattice of dimers ($d_\perp=\sigma_1$, $d_\parallel=\sigma_1+\sigma_0$, $\rho=2\sigma_0^2/[\sigma_1(\sigma_0+\sigma_1)]=0.228$). The soft core of any dimer is in contact, with no overlapping, with the soft cores of adjacent dimers. Figure 1(d) shows a rectangular lattice of dimers ($d_\perp=\sigma_1$; $d_\parallel=(\sigma_1+3\sigma_0)/2$, $\rho=4\sigma_0^2/[\sigma_1(3\sigma_0+\sigma_1)]=0.291$). Along the axis, dimers' soft cores overlap, the edge of the soft core of any dimer being in contact with the hard core of the closest particle of the adjacent dimer. In direction orthogonal to the dimer axis the soft cores of adjacent dimers are in contact with no overlapping. Figure 1(e) shows a triangular lattice of trimers ($\rho=2\sqrt{3}\sigma_0^2/[\sqrt{\sigma_1^2-(\sigma_0/2)^2}+\sqrt{\sigma_0^2-(\sigma_0/2)^2}]=0.315$). The soft core of each trimer is in contact with the soft cores of surrounding trimers, with no overlapping. Figure 1(f) shows a square lattice of dimers ($d_\perp=d_\parallel=\sigma_1$, $\rho=2(\sigma_0/\sigma_1)^2=0.32$). Along the axis, dimers' soft cores overlap, the edge of the soft core of any dimer being in contact with the edge of the corona of the less close particle of the adjacent dimer. A different arrangement is possible at the same density, namely the rectangular lattice of particles shown in Fig. 1(g) ($d_\perp=\sigma_1$; $d_\parallel=\sigma_1/2$). In this case, particles are disposed along parallel lines, the corona of each particle overlapping with the coronas of adjacent particles within the same line, with its edge in contact with the edge of the coronas of the second-neighbors particles. The coronas of particles belonging to adjacent lines are in contact with no overlapping. Figure 1(h) shows a rectangular lattice of particles ($d_\perp=\sigma_1$; $d_\parallel=\sigma_0$, $\rho=\sigma_0/\sigma_1=0.4$). The hard core of each particle is in contact with the hard cores of adjacent particles within the same line, while the coronas of particles belonging to adjacent lines are in contact with no overlapping. This is the densest configuration attainable without overlapping of coronas in a direction perpendicular to the line on which particles are disposed.

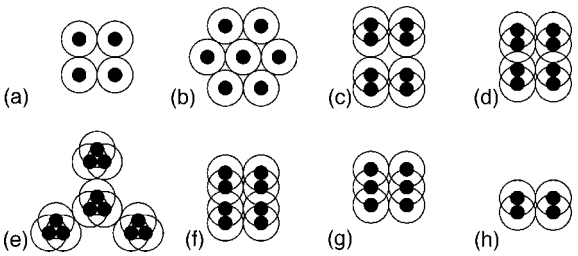

FIG. 1. Geometrical arrangements corresponding to densities: from left to right—(a) $\rho=0.16$; (b) 0.184; (c) 0.228; (d) 0.291; (e) 0.315; (f) 0.32; (g) 0.32; (h) 0.4.

Some of the configurations illustrated are specific of the adopted choice of σ_0 and σ_1. For example for $R=2$, the arrangements shown in Figs. 1(f) and 1(h) coincide.

IV. RESULTS AND DISCUSSION

MC simulations at constant number of particles N, volume V, and temperature T (*NVT* simulations) [26] showed [8] that at a fixed temperature, upon increasing the density, the system rapidly turns from a disordered configuration into a triangular lattice with few defects and lattice constant σ_1; then particles form dimers together with few short linear chains. Subsequently, dimers and particles align in wormlike filaments and eventually form stripe domain patterns similar to those exhibited by 2D real systems [27–29], while at even higher densities, the system is composed mainly of loose aggregates of three or more particles. The packing fractions at which these arrangements appear [8] are generally in

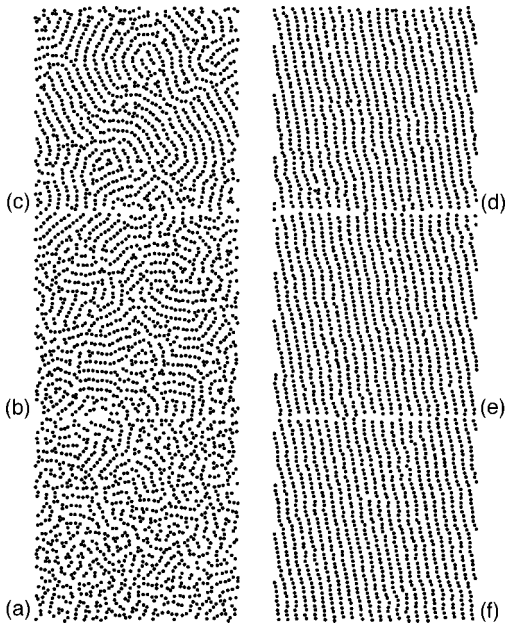

FIG. 2. Snapshots showing spatial configurations at $\rho=0.291$ and several temperatures. Left column, bottom to top: (a) $T=0.25$; (b) 0.20; (c) 0.19. Right column, top to bottom: (d) 0.18; (e) 0.17; (f) 0.15.

good agreement with those estimated from the previous geometrical analysis.

In particular, at $\rho=0.291$, the system exhibits remarkable stripe domains. In order to better understand the mechanism that leads to this intriguing feature, we investigated the stripe formation process at this density through an accurate annealing procedure: the system is initially disordered at high temperature and then brought from $T=0.3$ to 0.2 with temperature steps of 0.025 and from $T=0.2$ to 0.15 with steps of 0.01.

Figure 2 shows snapshots taken at several temperatures along the annealing isochore. As T_s is approached from above, particles gradually dispose themselves so to form winding filaments [$T=0.19$, Fig. 2(c)]. At a temperature $T_s(0.18<T_s<0.19)$, the system undergoes a rather sharp transition from a disordered state to a lamellar phase. At $T=0.18$ particles form nearly perfectly parallel straight stripes which span the whole system [Fig. 2(d)]. Upon further cooling, the few residual defects gradually disappear [Figs. 2(e) and 2(f)].

The pair distribution function $g(r)$, shown in Fig. 3, illustrates clearly that at the transition a relatively long-range order appears. In fact, below T_s, the distribution function is characterized by the persistence of the secondary peaks, which decrease much more slowly than in the disordered phase. We further analyze the structural order of our system through the structure factor $S(k)$, a quantity which represents a measure of density correlations in the wave vector space. The position $k_{\max}$ of the main peak of the structure factor provides an estimate of the length scale L which characterizes the structural order of the system ($k_{\max}\approx 2\pi/L$). As shown in Fig. 4, the first and the second peak, centered, respectively, at $k\gtrsim 2\pi/\sigma_1$ and at $k\gtrsim 2\pi/\sigma$, with

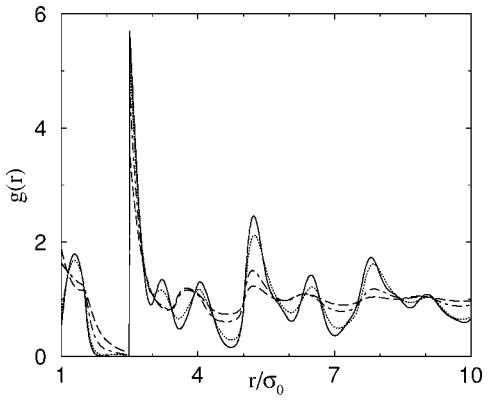

FIG. 3. Pair distribution function $g(r)$ at $\rho=0.291$ and $T=0.25$ (dashed line), 0.19 (dot-dashed line), 0.18 (dotted line), 0.15 (full line).

$\sigma_0<\sigma<\sigma_1$, increase considerably below the transition to the stripe phase. In particular, the growth of the second peak reveals that, in addition to σ_1, a new length scale, smaller than σ_1 but larger than σ_0, becomes effective below T_s. To interpret this result one must consider that at low temperatures, provided density is not too high, coronas are scarcely penetrable and the system behaves as an assembly of hard disks of effective diameter σ_1, with the ensuing dominance of the first peak. However, at the density considered, there is not enough space to accommodate all particles without interpenetrating of coronas. In fact, the low temperature stripe phase is characterized by penetration of the soft core along the stripes. The effective repulsive lengths are then the inner hard core in direction parallel to the stripes and the external corona radii in direction orthogonal to them. From the consequent competition between these two scales an intermediate effective length scale emerges, as reflected in the growth, in the structure factor, of the peak centered at $k\gtrsim 2\pi/\sigma$.

The self-organization principle which underlies the formation of the patterns observed is strictly related to the form of the interaction potential. In the presence of pure excluded volume interactions, the structural arrangement of the particles is driven by the requirement of maximizing the configurational entropy. An example is provided by crystallization of hard spheres. This system forms a stable HCP crystal.

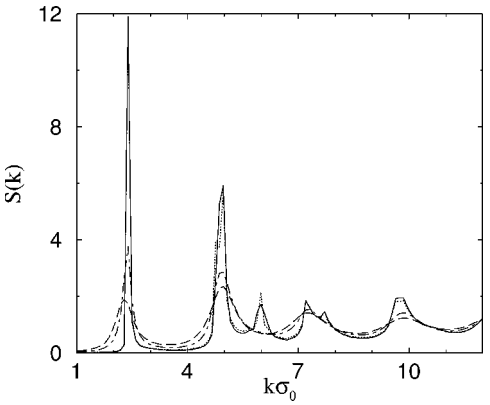

FIG. 4. Structure factors $S(k)$ at $\rho=0.291$ and $T=0.25$ (dashed line), 0.19 (dot-dashed line), 0.18 (dotted line), 0.15 (full line).

The solid phase has a greater entropy with respect to the fluid one: in fact an ordered structure such as the HCP crystal ensures that each particle has around itself enough space to sample through vibrational motions. As a consequence, in the solid phase a greater number of microstates is available to the system with respect to a disordered fluid phase (at the same density).

When the hard core is dressed with a soft shoulder, as in our case, the system has to obey, together with the maximum entropy rule, also a minimum energy requirement. In fact, when particles come sufficiently close, soft shoulders overlap: this implies an energetic cost which the system tries to minimize. If density is low, the system can satisfy both the maximum entropy and minimum energy rules simply by arranging particles on an ordered lattice in which they are at a distance from each other such that there is no overlapping of shoulders. At higher density (in our model, when $\rho > 0.184$, reduced units) this is no more possible. It is easy to realize that in this case a structure in which particles are equally spaced from each other would *maximize* the energetic cost for the system since the shoulder of each particle overlaps with those of all its nearest neighbors. Alignment of the particles (and at smaller densities, formation of dimers) allows one to minimize the number of overlaps and, accordingly, the energetic cost of the configuration. In these conditions, the spatial arrangement of the particles in our model is determined by a tradeoff between the two incompatible requirements of maximizing entropy and minimizing energy [30,31]. The deriving unavoidable frustration may have remarkable consequences. In particular, in the stripe configuration, in spite of the isotropic nature of the interaction pair potential, the soft repulsion is easily overcome along the stripes but not transversally to them. Thus, coronas act as efficient spacers between stripes, setting the pattern periodicity, but not between particles within the same stripe.

To check the robustness of the transition to the stripe phase, we performed an annealing procedure using also MC simulations at constant number of particles, temperature, and pressure P (*NPT* simulations) [26]. This simulation scheme allows volume to fluctuate and during the annealing procedure, at difference from *NVT* simulations, volume (or density) changes to keep pressure constant (in our calculations pressure is chosen so that around T_s the average density is close to 0.29). The results obtained, not reported here for brevity, show that around T_s the system undergoes a transition to an orientationally ordered phase in which particles are localized along linear domains. These results are in substantial agreement with our previous findings and confirm the formation of the stripe phase at low temperature.

V. DEPENDENCE ON POTENTIAL PARAMETERS

As discussed above, the essential feature responsible for stripe formation is, in our system, the competition between the hard and soft repulsions. Thus, we expect that the phenomenon keeps unaltered, at least qualitatively, also for different choices of the ratio between the hard and soft cores, provided that these two length scales are comparable with each other. To assess this point we investigate the behavior of our model for several values of R, with $R \geqslant 2$. Here we report the results relative to $R=2$; this choice is of particular interest since for this value of R a number of relevant configurations collapse into each other (as observed in Sec. II). The smaller soft core makes possible a tighter packing with respect to our previous choice. In particular, the geometrical arrangement shown in Fig. 1(d) corresponds now to the density $\rho=0.4$. We expect then that formation of stripes occurs at higher densities.

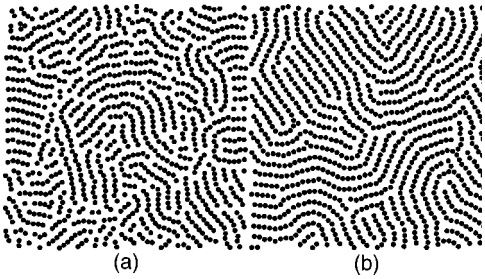

FIG. 5. Snapshots showing spatial configurations for $R=2$ at $T=0.1$: left to right—(a) $\rho=0.4$; (b) 0.45.

We perform *NVT* simulations at $\rho=0.4-0.45$ and $T=0.1$, disordering first the system at high temperature and then bringing it to the final temperature through three successive steps ($T=0.3, 0.2, 0.1$). We find that the spatial disposition (shown in Fig. 5) is characterized by the presence of winding filaments, similar to those exhibited at $\rho=0.291$ by the system with $R=2.5$ [see Fig. 2(d) of Ref. [8]].

Up to now we considered purely repulsive intermolecular interactions. However, attraction is often present, to a smaller or greater extent, in real systems due, for example, to dispersive terms or to depletion forces arising in mixtures of sufficiently asymmetric particles. Thus, a fundamental question is whether the formation of stripes occurs also in the presence of attraction. We introduce in the interparticle potential (for several radii ratios) an attractive component having the form of a well extending from $r=\sigma_1$ to $r=\sigma_1+\sigma_0/2$, with a number of attractive energies ($U_A=0.25, 0.5$). Here we show the results for $R=2$. The system with $U_A=0$ is first disordered at high temperature and then brought to $T=0.3$. Then attraction is progressively switched on. As shown in Fig. 6, attraction favors alignment of the particles. In fact, the transition to the stripe phase occurs at higher temperatures with respect to the purely repulsive interaction, the general features of the phenomenon being qualitatively unaltered.

Attraction appears then to enhance the capacity of the shouldered repulsive core to generate stripe patterns. This effect can be explained by considering that, at least for sufficiently dense configurations, the presence of attraction gives origin to a sort of line tension which stabilizes the stripes. On the microscopic side, the presence of the attractive well increases the average number of particles in the vicinity of the core (as shown by the radial distribution function reported in Fig. 7). This makes possible the penetration of the soft core, and thus the formation of stripes, at significantly higher temperatures. The robustness of stripe formation with respect to attractive forces widens considerably the applicability of the present analysis.

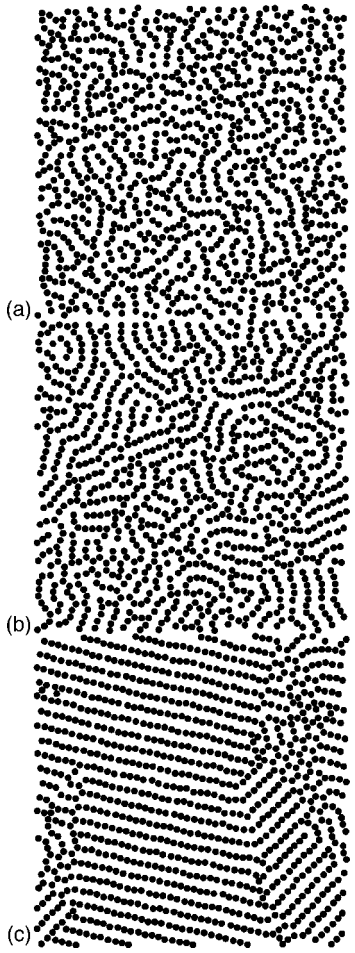

FIG. 6. Potential with attractive well ($R=2$). Snapshots showing spatial configurations at $T=0.3$ and $\rho=0.45$: top to bottom—(a) $U_A=0$; (b) 0.25; (c) 0.5.

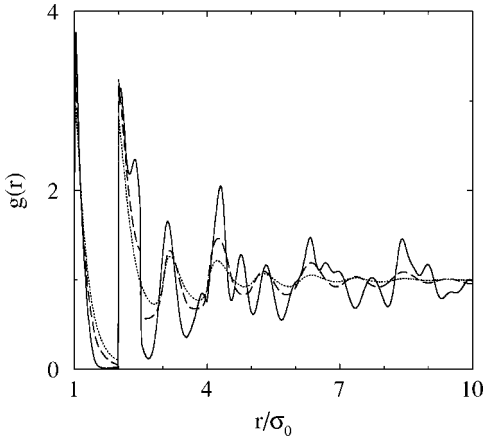

FIG. 7. Potential with attractive well ($R=2$). Pair distribution function $g(r)$ for $T=0.3$ and $\rho=0.45$: (a) $U_A=0$ (dotted line); (b) 0.25 (dashed line); (c) 0.5 (full line).

VI. CONCLUSIONS

We showed that 2D systems with core-corona architecture may spontaneously form stripe patterns. The physical mechanism underlying this phenomenon is to be found in the competition between the two length scales that characterize the repulsive component of the intermolecular interaction. The choice of the ratio between the hard and soft cores is not critical provided that they are comparable with each other. Thus, our findings are only weakly dependent on the specific choice of the model parameters, which enhances the relevance of the present study to real systems. We showed also that the stripe formation process is robust upon the introduction of an attractive component. Thus, core-corona potentials in the presence of attraction may give origin to stripe phases *and* to liquid-liquid first-order transitions [22], both unusual phenomena in simple model fluids. In the light of this result, a systematic investigation of the relation between the two phenomena in 2D real systems would be highly advisable. Indeed, some experimental results point in this direction, e.g., mixtures of lipids in monolayers, which exhibit stripe phases near a miscibility critical point [3].

In order to better understand the behavior of our model system a full knowledge of its phase diagram is necessary. We plan to undertake such an investigation in the near future. The results here reported open the possibility that a novel class of materials may be suited for the self-assembling of nanoscale structures. This technique may have many far-reaching technological applications. For example one day it could allow electronic devices to assemble themselves automatically, giving a way to mass-produce nanochips with circuit elements only a few molecules across.

[1] H. Mohwald, Thin Solid Films **159**, 1 (1988).
[2] M. Seul and R. Wolfe, Phys. Rev. A **46**, 7519 (1992).
[3] S. L. Keller and H. M. McConnell, Phys. Rev. Lett. **82**, 1602 (1999).
[4] J. Maclennan and M. Seul, Phys. Rev. Lett. **69**, 2082 (1992).
[5] C. Harrison *et al.*, Science **290**, 1558 (2000).
[6] M. Seul and D. Andelman, Science **267**, 476 (1995).
[7] A. D. Stoycheva and S. J. Singer, Phys. Rev. Lett. **84**, 4657 (2000).
[8] G. Malescio and G. Pellicane, Nat. Mater. **2**, 97 (2003).
[9] G. A. McConnel and A. P. Gast, Macromolecules **30**, 435 (1997).
[10] V. S. Balagurusamy, G. Ungar, V. Percec, and G. Johanson, J. Am. Chem. Soc. **119**, 1539 (1997).
[11] T. Cagin *et al.*, Comput. Theor. Polym. Sci. **11**, 345 (2001).
[12] G. Stell and P. C. J. Hemmer, Chem. Phys. **56**, 4274 (1970).
[13] P. G. Debenedetti, *Metastable Liquids: Concepts and Principles* (Princeton University Press, Princeton, 1998).
[14] P. T. Cummings and G. Stell, Mol. Phys. **43**, 1267 (1981); E. Velasco, L. Mederos, G. Navascues, P. C. Hemmer, and G. Stell, Phys. Rev. Lett. **85**, 122 (2000); J. M. Kincaid, G. Stell, and C. K. Hall, J. Chem. Phys. **65**, 2161 (1976).
[15] M. Silbert and W. H. Young, Phys. Lett. **58A**, 469 (1976); D. Levesque and J. J. Weis, *ibid.* **60A**, 473 (1977); J. M. Kincaid

and G. Stell, *ibid.* **65A**, 131 (1978); A. Voronel, I. Paperno, S. Rabinovich, and E. Lapina, Phys. Rev. Lett. **50**, 247 (1983).
[16] J. M. Lawrence, M. C. Croft, and R. D. Parks, Phys. Rev. Lett. **35**, 289 (1975).
[17] S. H. Behrens, D. I. Christl, R. Emmerzael, P. Schurtenberger, and M. Borkovec, Langmuir **16**, 2566 (2000); D. Wei and G. N. Patey, Phys. Rev. Lett. **68**, 2043 (1992).
[18] P. G. Debenedetti, V. S. Raghavan, and S. S. Borick, J. Phys. Chem. **95**, 4540 (1991).
[19] F. H. Stillinger and T. Head-Gordon, Phys. Rev. E **47**, 2484 (1993); F. H. Stillinger and D. K. Stillinger, Physica A **244**, 358 (1997).
[20] M. R. Sadr-Lahijany, A. Scala, S. V. Buldyrev, and H. E. Stanley, Phys. Rev. Lett. **81**, 4895 (1998); Phys. Rev. E **60**, 6714 (1999); A. Scala, M. R. Sadr-Lahijany, N. Giovambattista, S. V. Buldyrev, and H. E. Stanley, *ibid.* **63**, 041202 (2001).
[21] G. Franzese, G. Malescio, A. Skibinsky, S. V. Buldyrev, and H. E. Stanley, Nature (London) **409**, 692 (2001).
[22] G. Malescio and G. Pellicane, Phys. Rev. E **63**, 020501 (2001).
[23] E. A. Jagla, Phys. Rev. E **58**, 1478 (1998); **63**, 061501 (2001); J. Chem. Phys. **111**, 8980 (1999).
[24] S. Buldyrev, G. Franzese, N. Giovambattista, G. Malescio, M. R. Sadr-Lahijany, A. Scala, A. Skibinsky, and H. E. Stanley, Physica A **304**, 23 (2002).
[25] The densest arrangement possible for hard disks of diameter σ is a close-packed two-dimensional triangular lattice. This fills a fraction $\eta_{cp}=\sqrt{3}\pi/6=0.9069$ of the total space. This number follows from the ratio of the area of the disk to the area of the circumscribing hexagon whose side equals $\sigma/\sqrt{3}$. Since the packing fraction in two dimensions is $\eta=1/4\pi\rho\sigma^2$ it follows that the close-packed density is $\rho_{cp}\sigma^2=2/3\sqrt{3}=1.153$. The density of a close-packed two-dimensional triangular lattice of hard disks of diameter $\sigma_1=2.5$ is then $\rho=2/3\sqrt{3}/(\sigma_1/\sigma_0)^2 \approx 0.184$.
[26] D. Frenkel and B. Smit, *Understanding Molecular Simulation* (Academic, London, 1996).
[27] R. M. Weis and H. M. McConnell, Nature (London) **310**, 47 (1984).
[28] T. A. Witten Phys. Today **21**, 21 (1990).
[29] J. Hahm, W. A. Lopes, H. M. Jaeger, and S. J. Sibener, J. Chem. Phys. **109**, 10111 (1998).
[30] P. Ziherl and R. D. Kamien, Phys. Rev. Lett. **85**, 3528 (2000).
[31] P. Ziherl and R. D. Kamien, J. Phys. Chem. B **105**, 10147 (2001).